ingegneria sismica
International Journal of Earthquake Engineering
Anno XLIII - Num. 2 - 2026

Optimizing Collaborative Efficiency in Tourism Supply Chains: An Intelligent Decision-Making Approach

Fanfan Kong[1], *Junling Wen*[1] *and Huiqi Zhang*[2,*]

[1] Economics and Management School, Binzhou Polytechnic University, Binzhou 256603, Shandong, China

[2] School of Tourism Management, Zhuhai City Polytechnic, Zhuhai, 519090, Guangdong, China

SUMMARY: *This research carries out investigation on optimization of collaborative efficiency inside tourism supply chains, in which scenic spots, hotels, transport suppliers, online travel agents, catering and retail services, and tourist demand nodes interact with each other under fluctuant demand and time-sensitive capacity restriction conditions. One heterogeneous tourism supply-chain graph has been constructed, it is used for representing transaction relations, spatial closeness, capacity mutual complementarity, and disturbance spread. According to this graph, one intelligent decision-making model is established through integrating relation-conscious time requirement prediction, cooperative capability distribution, multi-agent movement selection, and constraint-conscious feasibility revision. We use public tourism statistics to carry out calibration work on the experimental dataset, and it is generated as daily operation samples that cover 12 destination cities in the period from 2019 to 2025. We have carried out comparison experiments with the Static CPFR, ARIMA-LP, LSTM-Heuristic, GNN-Optimizer, and MARL-CPFR baseline methods. The experiment results indicate that the method which we put forward obtains a MAPE of 6.52%, a service fulfillment rate of 95.1%, a capacity utilization rate of 82.4%, and a collaborative operation efficiency index of 89.6. When put in comparison with the best-performing baseline method, the method that we put forward makes forecasting error decrease by 12.0%, makes COEI rise by 4.9 points, and makes average response delay become shorter by 28.2%. Scene experiments further prove that our method still keeps stability under weekend peak flows, weather interferences, festival peak crowds, transportation limits, and combined interferences. The research results indicate that graph-based intelligent decision-making method can promote the conversion of demand prediction accuracy into implementable cooperative actions, hence providing operation support for destination management platforms, OTA resource distribution, and tourism emergency coordination work.*

KEYWORDS: *tourism supply chain; collaborative efficiency; intelligent decision-making; graph neural network; multi-agent coordination*

1 Introduction

The synergetic effect efficiency of the tourism supply chain, first of all, it is reflected on the reception ability at the destination place. Tourists finish the road, living place, traffic and ticket grouping via OTA platform before they go to travel, and furthermore keep on producing food,

*aiq28@live.com
https://doi.org/10.65102/is2026769
Published: 30 April, 2026

connection, second spending, temporary change of visa and travel road adjustment after they come to the destination. For single operation units, these requirements show themselves as order quantities, room bookings, travel arrangements, waiting line numbers or stock changes; To the destination places, they as a whole constitute a dynamic supply network that spans scenic spots, hotels, traffic means, eating shops, platforms and ground handling service suppliers. The report of UN Tourism puts forward that the whole world's international tourist arrivals in the year 2025 will be about 1.52 billion, which is an increase of close to 60 million compared with the year 2024[1]. The economic influence research of WTTC also indicates that tourism will provide support for 366 million work positions in 2025 [2]. In the high base recovery stage, destination operation works have changed from simple hospitality service to finely adjusted cooperation, therefore, supply chain efficiency has the direct influence on tourist experience, enterprise income, and region bearing ability.

Inventories of tourism services have obvious time period attributes. Hotel rooms, scenic area capacity, transportation seats, tour guide services and food and beverage reception capacity are all constrained by specific dates and specific time periods, and unused capacity is difficult to preserve across time. In contrast to manufacturing supply chains, tourism supply chains are also affected by a combination of weather, holidays, activity events, traffic congestion, and social media buzz. Tourist demand may shift from normality to a concentrated influx in a short period of time, while the supply side is constrained by physical capacity, service windows, and organizational boundaries that prevent simultaneous expansion. If each entity makes localized decisions based only on its own orders, it is prone to problems such as long queues at popular scenic spots, mismatches between remaining hotel rooms and transportation seats, unused food and beverage reception capacity, and platform recommendations that continue to exacerbate congestion. The core of such phenomena is not the lack of capacity of individual links, but the lack of synergy between demand forecasting, capacity allocation, information sharing and dynamic response.

AI and digitization provide a new technological foundation for tourism supply chain synergies.The OECD, in its G7/OECD policy paper, states that AI can be used for tourism innovation and sustainable development, while needing to deal with data governance and risk constraints between firms, destinations, and governments [3].Ku discusses the role of tourism digitization on product advantage and supply chain competition from the perspective of digital capabilities and real options theory [4]; Bekele and Raj's bibliometric study shows that tourism digitization has expanded from a single information system application to platforms, data governance, and smart service scenarios [5]; Luu et al. further introduce Industry 4.0 technologies into tourism supply chain research, emphasizing the linkages between platform interconnectivity, smart technologies, and supply chain resilience [6].Sarfraz et al. analyze sustainable supply chain, digital supply chain and supply chain competitiveness based on a hotel and resort sample analyzed the impact of sustainable supply chains, digital transformation and blockchain adoption on the competitive advantage of tourism firms [7]. These studies illustrate that the tourism supply chain is no longer just a collection of business transactional relationships, but a collaborative network driven by a combination of data, platforms, resource capacity and real-time demand.

Existing research still suffers from three issues that directly affect deployment. First, tourism supply chain collaboration is often treated as a static collaboration or resilience evaluation problem, with insufficient portrayal of the heterogeneous relationships among scenic spots, hotels, transportation, OTAs, and tourists' demands.Erol et al. constructed a driver and constraint framework for supply chain resilience in tourism and hospitality [8], and Zheng assessed the resilience of tourism supply chains based on complex networks and genetic algorithms [9]; however, such researches are more biased towards structural assessment, the

under-expression of demand shifting and capacity reallocation in rolling operations. Second, demand forecasting is often separated from resource decision making. Graph neural networks, Transformer and spatial deep learning have been used for tourism demand forecasting [10], but there is still a lack of a unified mechanism for how the forecast results enter cross-principal capacity allocation, order diversion and response actions. Third, there is a realistic boundary for multi-subject data sharing. The system interfaces, commercially sensitive data and response rhythms of hotels, platforms, transportation and scenic spots are not consistent, the governance cost of fully centralized scheduling is high, and simple distributed rules are difficult to avoid local optimum.

Therefore, this paper focuses on the optimization of cooperative operation efficiency of tourism supply chain, and constructs an intelligent decision-making method for heterogeneous subject networks. The study organizes scenic spots, hotels, transportation, OTAs, catering retail and tourists' demands into heterogeneous graph structures, on the basis of which graph time-series demand prediction, collaborative capacity allocation and constraint-aware action correction are carried out. The contribution of this paper is reflected in three aspects. First, it establishes a heterogeneous graph representation of the tourism supply chain, which integrates transaction intensity, capacity complementarity, space time cost and disturbance risk uniformly into the side-weight construction. Second, a demand forecasting and collaborative decision linkage model is proposed so that the forecasting results can be directly translated into capacity allocation, order diversion and service response actions. Third, rolling simulation experiments and multi-perturbation scenario comparisons are set up to test the improvement of this paper's method in forecasting accuracy, service fulfillment, capacity utilization, response delay, synergy cost, and comprehensive efficiency.

2 Methods

2.1 Data construction and tourism supply-chain graph representation

This thesis uses a data building way that joins public statistics data rectification and destination running sample imitation. The macro scope refers to the international tourism recovery and tourism economy influence data that are issued by UN Tourism and WTTC, and the destination samples are chosen from 12 typical tourism cities, which cover four kinds of tourism scenes: seashore rest, cultural inheritance, mountain holiday and city view watching. The monthly demand sequence includes 2019-2025, and the daily granularity operation sample is produced through the destination seasonal coefficients, holiday influences, weather disturbances, transportation conditions and platform search temperature. This design does not make the assumption that real order data at the enterprise level can be completely shared, hence it is applicable to the collaborative decision verification of travel supply chains which have relatively strong multi-subject data boundaries.

The cleaned experimental samples include 436 supply chain nodes, 5,218 collaborative edges, 86,400 daily granular demand records and 31,104 supply capacity records. The nodes are classified into 6 categories: scenic nodes, hotel nodes, transportation nodes, OTA nodes, food and beverage retail nodes, and tourist demand nodes. Edges are categorized into 4 types: transaction edges, spatial proximity edges, complementary capacity edges, and perturbation conduction edges. Transaction edges reflect the order or flow conversion relationship, spatial proximity edges reflect the cost of movement within the destination, capacity complementary edges reflect the degree of match between hotel, transportation, scenic spot and catering reception capacity, and perturbation conduction edges reflect the diffusion of the impact of

weather, traffic congestion, and activity events on neighboring nodes. The experimental data structure and variable definitions, as shown in Table 1.

Table 1: Experimental data structure and variable definition

Data Object	Number or Value	Description
Destination Cities	12	Covers coastal, mountainous, cultural heritage, and urban leisure destinations
Total Nodes	436	Scenic spots, hotels, transportation, OTAs, dining retail, and tourist demand
Total Collaboration Edges	5,218	Transactions, spatial proximity, capacity complementarity, disturbance propagation
Monthly Demand Series	84	Periods from 2019 to 2025
Daily Granularity Demand Samples	86,400	Order volume, visitor flow, search popularity, and visit probability
Supply Capacity Records	31,104	Room availability, seating capacity, reception limits, and business hours
Disturbance Variables	5	Weather, holidays, event occurrences, traffic conditions, and price fluctuations
Data Division	2019—2023 / 2024 / 2025	Training set, validation set, test set

Publicly available statistics, destination operational variables and multi-agent synergistic relationships are uniformly organized into a heterogeneous supply chain diagram as shown in Figure 1.

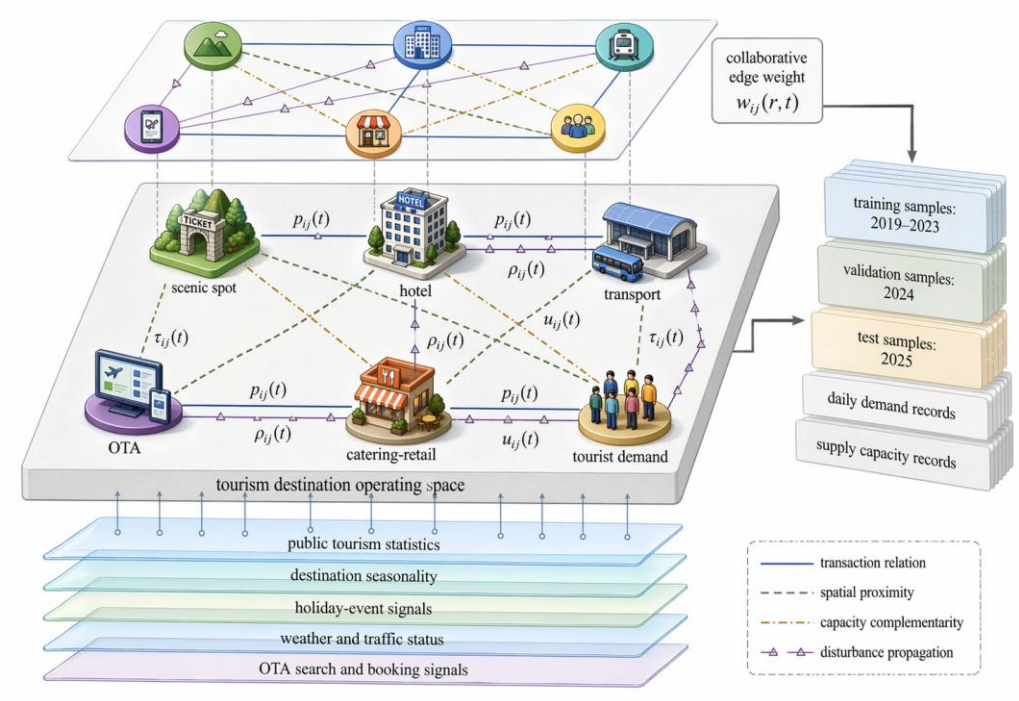

Figure 1: Tourism supply-chain graph representation and sample construction mechanism.

Edge weights are used to express the synergy intensity between different subjects. In this paper, transaction intensity, capacity complementarity, space time cost and disturbance risk are included in the unified mapping as shown in equation (1).

$$w_{ij}^{(r,t)} = \sigma\left(\beta_0 + \beta_1 p_{ij}^{(t)} + \beta_2 u_{ij}^{(t)} - \beta_3 \tau_{ij}^{(t)} - \beta_4 \rho_{ij}^{(t)}\right) \quad (1)$$

where $w_{ij}^{(r,t)}$ denotes the synergy edge power between node i and node j in time period t under relationship type r; $\sigma(\cdot)$ is the normalized mapping function; β_0 to β_4 are parameters calibrated by empirical proof sets; $p_{ij}^{(t)}$ denotes the transaction or order transformation intensity; $u_{ij}^{(t)}$ denotes the degree of capacity complementarity; $\tau_{ij}^{(t)}$ denotes the space time cost; and $\rho_{ij}^{(t)}$ denotes the perturbation risk. This formula gives higher marginal weights to relationships with high transaction intensity and high capacity complementarity, while suppressing synergistic relationships that are too far away, have high transfer costs, and have high perturbation risks.

Edge weights are updated using a rolling daily granularity. Platform search heat, weather warnings, traffic congestion and festivals change the short-term synergy intensity between nodes. For example, if the search heat of a scenic spot increases but the traffic congestion increases, the transaction intensity term increases, and the space time cost and disturbance risk increase simultaneously, and whether the final edge weight increases or not depends on the relative strength of the two types of factors. This process enables the model to identify nodes with “hot demand but can't continue to attract traffic”, and also to find alternative nodes with “average demand but can take transfer traffic”. Compared with the static adjacency matrix, the dynamic edge weights are more suitable for expressing the structural changes of the tourism supply chain under holidays, weather disturbances and traffic control.

2.2 Intelligent collaborative decision model

According to the construction of heterogeneous graph, the model of this paper is composed of four parts: graph time sequence prediction, cooperative capability distribution, multi-subject behavior decision and constraint revision. The module of graph time sequence prediction undertakes the responsibility to estimate the pressure of every demand node and service node in the coming 48 hours. The module for cooperative capacity allocation produces the preliminary resource distribution on the basis of the forecasted demand, service ability, and side-right relations. The multi-discipline action choosing module lets scenic spot, hotel, traffic and platform nodes pick doable actions under partial restriction conditions. The constraint correction module carries out callback processes for overcapacity, overtime window, and over-adjustment high-cost actions. Spatio-temporal depth study study and graph nerve networks have been proven by people to catch multi-attraction, multi-region demand connections in tourism demand prediction [11-14]; Studies of supply chain graph learning have also given the illustration that graph structures can be utilized to discover hidden synergic relations and promote the visibility of supply chains [15, 16]. The current paper therefore builds on these fundamental foundations through directly embedding graph forecasting results into the operational decision making hierarchical layer. The graph temporal encoder which considers relationships, is shown in equation (2).

$$h_i^{(t)} = GRU\left(h_i^{(t-1)}, \sum_{r\in\mathcal{R}} \sum_{j\in\mathcal{N}_i^r} \alpha_{ij}^{(r,t)} x_j^{(t)} W_r\right), \quad \hat{d}_i^{(t+1)} = Softplus\left(h_i^{(t)} v + b\right) \quad (2)$$

where $h_i^{(t)}$ denotes the hidden state of node i at time period t; $GRU(\cdot)$ is used to preserve the time dependence of the demand sequence; $\mathcal{R}$ denotes the set of relationship types; $\mathcal{N}_i^r$ denotes the set of neighbors of node i under relationship r; $\alpha_{ij}^{(r,t)}$ denotes the attention weight; $x_j^{(t)}$ denotes the input characteristics of node j; W_r is the mapping matrix corresponding to the relationship types; $\hat{d}_i^{(t+1)}$ denotes the predicted demand at the next time period; and v and b are the parameters of the output layer. ensure that the predicted demand is non-negative. The encoder maps different edge types separately so that transaction edges, capacity complementary edges and perturbation conduction edges are not compressed into the same neighborhood. The synergistic capacity allocation transforms the predicted demand into an executable resource allocation as shown in equation (3).

$$\min_{\mathbf{y}^{(t)}} J^{(t)} = \sum_{i\in\mathcal{D}}\left(c_i^o o_i^{(t)} + c_i^s s_i^{(t)} + c_i^m m_i^{(t)}\right) + \lambda \sum_{(i,j)\in\mathcal{E}} z_{ij}^{(t)} \tag{3a}$$

$$o_i^{(t)} \geq \hat{d}_i^{(t)} - y_i^{(t)}, \quad s_i^{(t)} \geq y_i^{(t)} - q_i^{(t)}, \quad 0 \leq y_i^{(t)} \leq q_i^{(t)} \tag{3b}$$

where $\mathbf{y}^{(t)}$ denotes the cooperative allocation scheme for time period t; $J^{(t)}$ is the integrated operational loss; $\mathcal{D}$ denotes the set of demand-related nodes; c_i^o, c_i^s, and c_i^m denote the unit cost of unmet demand, overcapacity pressure, and cross-node transfer adjustment, respectively; $o_i^{(t)}$ denotes the demand gap; $s_i^{(t)}$ denotes the amount of capacity overload; $m_i^{(t)}$ denotes the amount of cross-node transfer; λ denotes the cooperative adjustment penalty factor; $\mathcal{E}$ denotes the set of synergy edges; $z_{ij}^{(t)}$ denotes the synergy enablement cost on edges (i, j); $q_i^{(t)}$ denotes the available service capacity of a node. The constraints ensure that the allocation result does not exceed the node capacity and explicitly record the demand gap and capacity pressure.

Considering that travel supply chain subjects have local autonomy characteristics, this paper introduces a constraint-aware action selection mechanism. The mechanism draws on the idea of multi-intelligence body reinforcement learning in distributed inventory and supply chain disturbance processing [17, 18], but does not require all subjects to share the original order data. The action selection is shown in equation (4).

$$a_t^* = \arg\max_{a_t\in\mathcal{A}} [Q_\theta(s_t, a_t) - \eta\Omega(a_t) - \mu B(a_t)] \tag{4}$$

where a_t^* denotes the final action in time period t; $\mathcal{A}$ denotes the set of optional actions; $Q_\theta(s_t, a_t)$ denotes the expected revenue of action a_t in state s_t; $\Omega(a_t)$ denotes the extent to which the action violates the capacity, service window, or business boundaries; $B(a_t)$ denotes the cross-subjective adjustment burden triggered by the action; and η and μ are penalty weights. The mechanism enables the model to exclude non-deployable actions in the execution phase, such as continuing to allocate orders to full-roomed hotels, continuing to divert traffic to traffic-constrained scenic spots, and additional service requests outside the business hours. The model in this paper connects graph timing prediction, capacity co-allocation, and action feasibility correction as a closed-loop decision-making mechanism, as shown in Fig. 2.

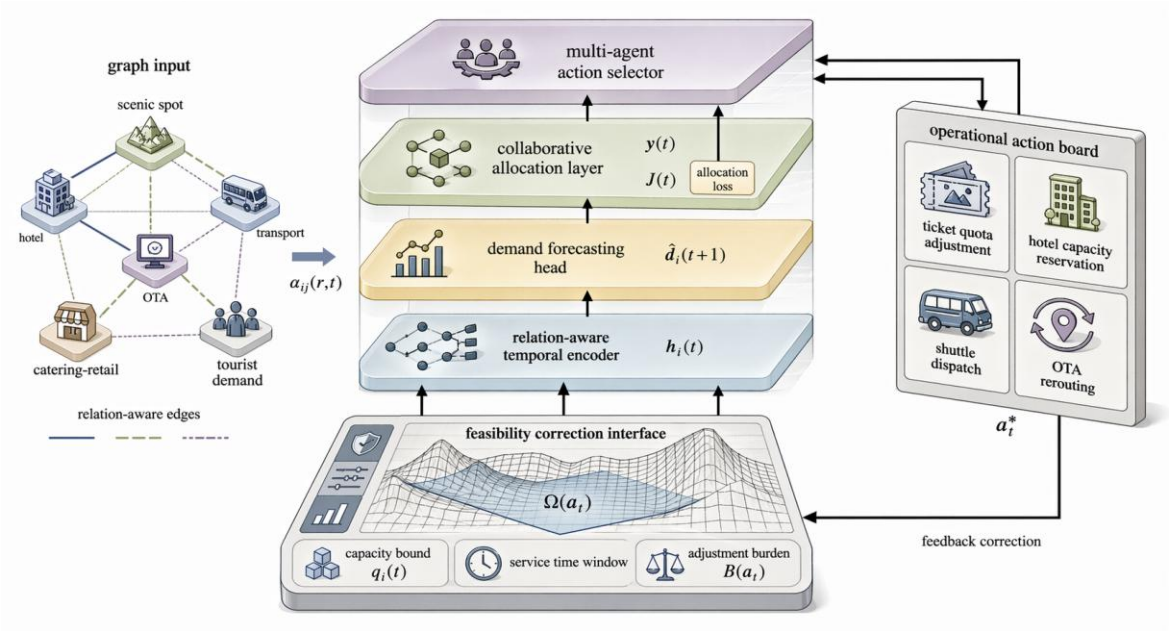

Figure 2: Constraint-aware intelligent collaborative decision mechanism.

In the model training stage, the parameters are updated by using weighted objectives for prediction mistakes and operation losses, and in the execution stage, new data are read and actions are corrected by using a rolling window. In comparison with the traditional CPFR method [19, 20], the approach that this paper puts forward keeps the thought of cooperative forecast and shared arrangement plans, but it substitutes the static arrangement for dynamic side weights, graph time forecast, and constraint-conscious action choice. This difference is the main source that brings follow-up efficiency promotion.

2.3 Experimental protocol and evaluation indicators

Our experiments have adopted a rolling forecast and rolling decision working protocol. The samples of 2019 to 2023 are utilized for the training work, the samples of 2024 are utilized for parameter adjustment, and the samples of 2025 are utilized for the testing work. Each rolling decision makes reading of the history window from past 24 hours, and outputs the demand forecast and the co-allocation plan for coming 48 hours. This model carries out the update of the demand forecast and the co-allocation scheme in every six hours. This model, every 6 hours, carries out the update work for the side weights, the demand forecasts, and the action correction results. This model is utilized in the experiments that use the same data division and the same rolling data division, and the same rolling data division. Our experiments adopt identical data partitioning, identical rolling window and identical evaluation indicators, hence to prevent the comparison methods from producing deviation that is caused by the difference of sample windows. Our experiments adopt rolling prediction and rolling decision schemes to reduce the influence of one-time static partitioning on efficiency assessment, which is displayed in Fig. 3.

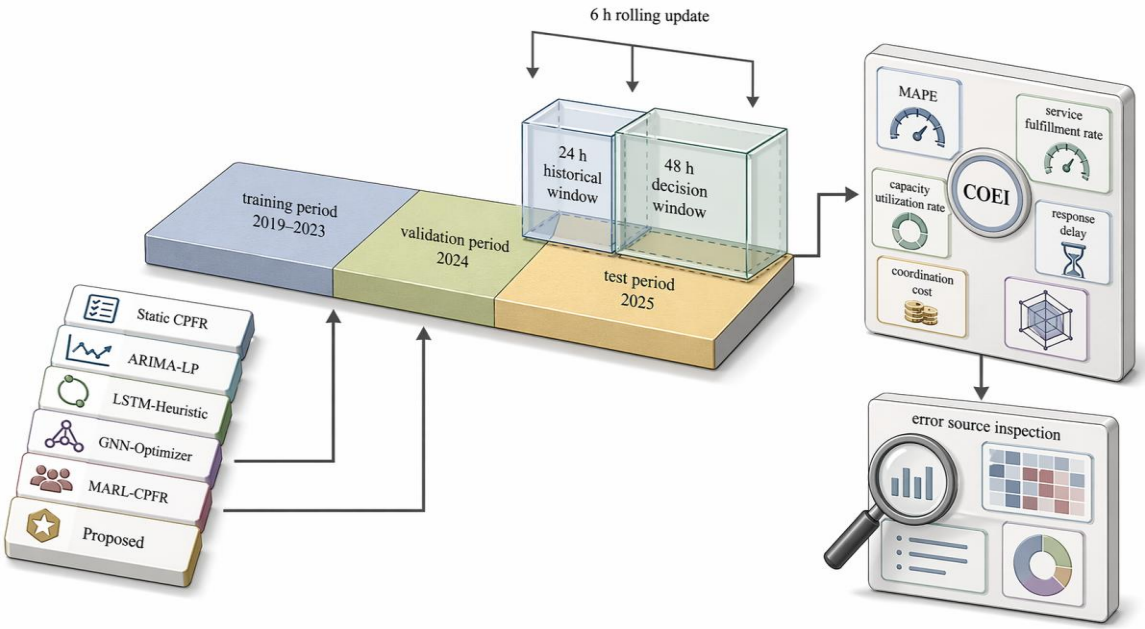

Figure 3: Rolling experiment and evaluation protocol.

The comparison methods include five categories.Static CPFR denotes fixed collaborative planning and fixed replenishment rules.ARIMA-LP denotes time series prediction with linear programming allocation.LSTM-Heuristic denotes demand prediction is done with LSTM followed by heuristic capacity allocation.GNN-Optimizer denotes demand prediction is done using graph neural networks and resource allocation is done with an optimizer.MARL-CPFR denotes a joint model that introduces multiintelligents reinforcement learning into the heterogeneous graph time-series prediction and transfer action. MARL-CPFR denotes the introduction of multi-intelligence reinforcement learning into collaborative prediction and transfer actions.Proposed denotes the joint model of heterogeneous graph timing prediction, collaborative allocation and constraint-aware action correction proposed in this paper.

The evaluation metrics include MAPE, service fulfillment rate, capacity utilization rate, average response delay, unit order synergy cost, and comprehensive synergy operation efficiency index.MAPE is used to evaluate the demand prediction error; service fulfillment rate indicates the ratio of satisfied demand to total demand; capacity utilization rate indicates the ratio of service capacity being effectively used; average response delay indicates the average time from the identification of the demand change to the completion of the execution of the action; and the average response delay includes the time from the identification of the demand change to the completion of the execution of the action. average time; unit order coordination cost includes transfer subsidy, connection adjustment, platform diversion and temporary scheduling cost. Comprehensive efficiency index, as shown in equation (5).

$$\mathrm{COEI} = 100(0.35F + 0.25U + 0.20R + 0.20C) \tag{5}$$

where COEI denotes the comprehensive cooperative operation efficiency index; F denotes the normalized score of service performance rate; U denotes the normalized score of capacity utilization rate; R denotes the normalized score of response speed; and C denotes the normalized score of cooperative cost. The weights are set based on the operational objectives of the tourism supply chain, where service fulfillment is given the highest priority, capacity utilization and response speed are the second highest, and collaboration cost is used to constrain

excessive scheduling. All comparisons are averaged over the 12 destinations and the 2025 test sample, and a rolling window of results is used to calculate the final metrics.

3 Results and Discussion

3.1 Overall performance of collaborative efficiency optimization

This section first tests whether the method of this paper can improve the efficiency of tourism supply chain collaboration at an aggregate level. Since tourism supply chain operations are simultaneously affected by demand forecasting, capacity utilization, response rate, and synergy cost, comparing forecasting errors alone cannot account for operational improvements. Therefore, this paper includes MAPE, service fulfillment rate, capacity utilization, average response delay, unit order synergy cost and COEI in the comparison at the same time, and the results are shown in Table 2.

Table 2: Overall comparison of different collaborative decision methods

Method	MAPE / %	Service Fulfillment Rate / %	Capacity Utilization Rate / %	Average Response Delay / h	Unit Order Coordination Cost / CNY	COEI
Static CPFR	13.84	86.5	68.2	7.6	18.42	71.3
ARIMA-LP	11.27	88.1	70.6	6.2	17.85	74.9
LSTM-Heuristic	9.36	90.4	73.8	5.1	16.94	79.5
GNN-Optimizer	7.84	92.7	76.9	4.3	16.12	83.8
MARL-CPFR	7.41	93.2	78.1	3.9	15.87	84.7
Proposed	6.52	95.1	82.4	2.8	14.96	89.6

In Table 2, Static CPFR has a MAPE of 13.84%, a service fulfillment rate of 86.5%, and a COEI of 71.3, indicating that the fixed synergy rule has a significant lag in the face of peaks and valleys in demand fluctuations.ARIMA-LP reduces the MAPE to 11.27%, but its capacity utilization rate is only 70.6%, indicating that linear programming can improve the allocation results, but it is difficult to represent LSTM-Heuristic further reduces the MAPE to 9.36%, but its average response delay is still 5.1 h, reflecting that there is still a break between the forecasting module and the capacity allocation.GNN-Optimizer and MARL-CPFR achieve a COEI of 83.8 and 84.7, respectively, suggesting that graphical relational modeling and multi-subjective action selection can improve the synergy efficiency. indicate that both graph relationship modeling and multi-subject action selection can improve the synergy efficiency. The MAPE of this paper is 6.52%, which is 12.0% lower than the optimal baseline MARL-CPFR; the service compliance rate reaches 95.1%, the capacity utilization rate reaches 82.4%, the average response latency is reduced to 2.8 h, and the COEI reaches 89.6. The changes in efficiency and response latency of the different methods within the 48-h rolling decision window are shown in Fig. 4.

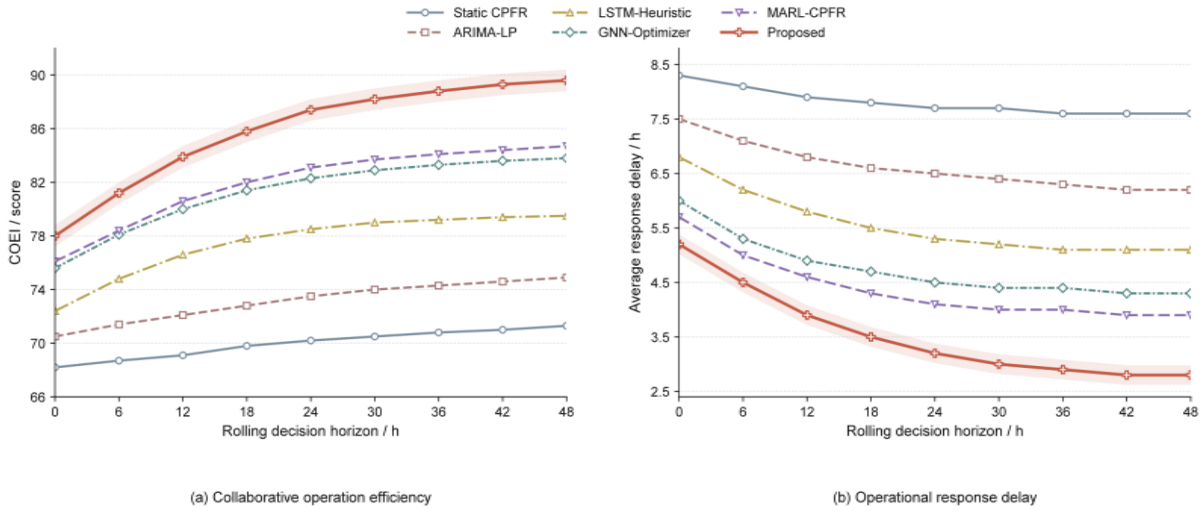

Figure 4: Rolling collaborative operation efficiency and response delay.

In Fig. 4, the COEI curve of Static CPFR rises slowly from 68.2 to 71.3, and the response latency always stays around 7.6 h, which indicates that the fixed synergy rule can only absorb the regular fluctuations, and the efficiency improvement of ARIMA-LP and LSTM-Heuristic is concentrated in the first 24 h, and then tends to be flat. The curves of GNN-Optimizer and MARL-CPFR enter the range of 83 points or above, but the response delay is still higher than 3.9 h. In this paper, the method reaches 87.4 at 24 h, 89.6 at 48 h, and the response delay is reduced to 2.8 h, which indicates that graphical modeling and constraints correction improve the speed of efficiency enhancement and the speed of action execution at the same time.

The overall results show that the advantages of this paper's method do not only come from the decrease of prediction error. If only the prediction accuracy is improved, it may still produce non-executable allocation schemes; if only multi-subject action selection is done, the model may lack the advance sensing of demand linkage. The method in this paper identifies the synergy relationship through heterogeneous edge weights, predicts the node pressure through graph timing module, and then filters the non-executable solutions through capacity and action constraints, and thus is able to simultaneously reduce the demand gap, compress the response time, and reduce the ineffective synergy cost. The unit order synergy cost is reduced from 15.87 CNY in MARL-CPFR to 14.96 CNY, indicating that the model does not trade off the fulfillment rate through high-frequency rescheduling or over-subsidization, but rather improves the supply-demand matching within the executable boundary.

3.2 Scenario robustness and ablation analysis

Travel supply chain synergy efficiency improvement in normalized scenarios is not sufficient proof that the model possesses deployment stability. Destination operations are often affected by weekend peaks, weather disturbances, festivals, transportation constraints, and the superposition of multiple disturbances. In order to test the stability of the model under different perturbations, this paper sets up six types of scenarios and compares the COEI of each method, and the COEI distribution of each method under different perturbation scenarios is shown in Fig. 5.

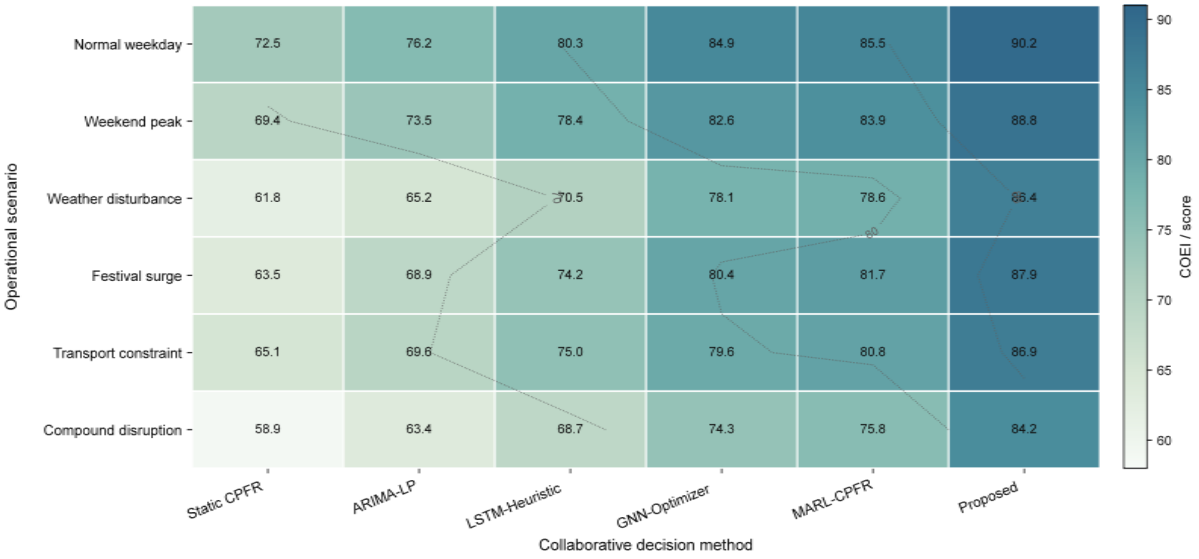

Figure 5: Scenario-specific efficiency heatmap under operational disturbances.

In Fig. 5, weather perturbation and composite perturbation are the two scenarios with the most obvious efficiency degradation. the COEI of Static CPFR under composite perturbation is only 58.9, and that of ARIMA-LP is 63.4, which indicates that Static Collaborative and Linear Programming lacks the adaptive ability to sudden changes in edge weights and capacity contraction. the GNN-Optimizer reaches 84.9 on normal weekdays but falls to 74.3 under composite perturbation. It drops to 74.3 under compound perturbations, indicating that graph prediction is still affected by sudden capacity changes if it lacks action layer constraints. The method in this paper maintains a score of 84 or above in all six scenarios, including 90.2 for normal working days and 84.2 for compound perturbations, showing that its efficiency advantage is not limited to smooth scenarios. The results of scenario robustness and ablation experiments are shown in Table 3.

Table 3: Scenario robustness and ablation results

Experimental Setup	MAPE / %	Service Fulfillment Rate / %	Capacity Utilization Rate / %	Response Delay / h	Constraint Violation Rate / %	COEI
Full model	6.52	95.1	82.4	2.8	1.9	89.6
w/o graph relation	7.38	93.0	78.5	3.3	2.6	86.0
w/o constraint correction	6.89	94.2	80.1	4.4	5.8	86.7
w/o MARL action selection	6.74	92.8	79.4	4.9	4.9	85.9
w/o disturbance features	7.06	93.7	80.5	3.7	3.1	87.5

In Table 3, after removing the graph relationship, MAPE rises from 6.52% to 7.38%, and capacity utilization decreases from 82.4% to 78.5%, indicating that heterogeneous edge weights have a direct role in identifying intra-destination demand linkages and capacity complementarities. After removing constraint corrections, MAPE only rises to 6.89%, but constraint violation rises to 5.8% and response delay increases to 4.4 h, indicating that prediction accuracy does not automatically translate into deployable solutions. After removing the multi-intelligent body action selection, the service compliance rate drops to 92.8% and the response delay rises to 4.9 h, reflecting the difficulty of centralized one-time allocation to adapt to local response differences in the multi-intelligent body autonomy environment. After

removing the perturbation feature, COEI decreases to 87.5, which is smaller than the previous types of ablation, but the decrease is more obvious in weather perturbation and traffic-constrained scenarios. The change in the performance of the COEI after the removal of the core module is shown in Fig. 7.

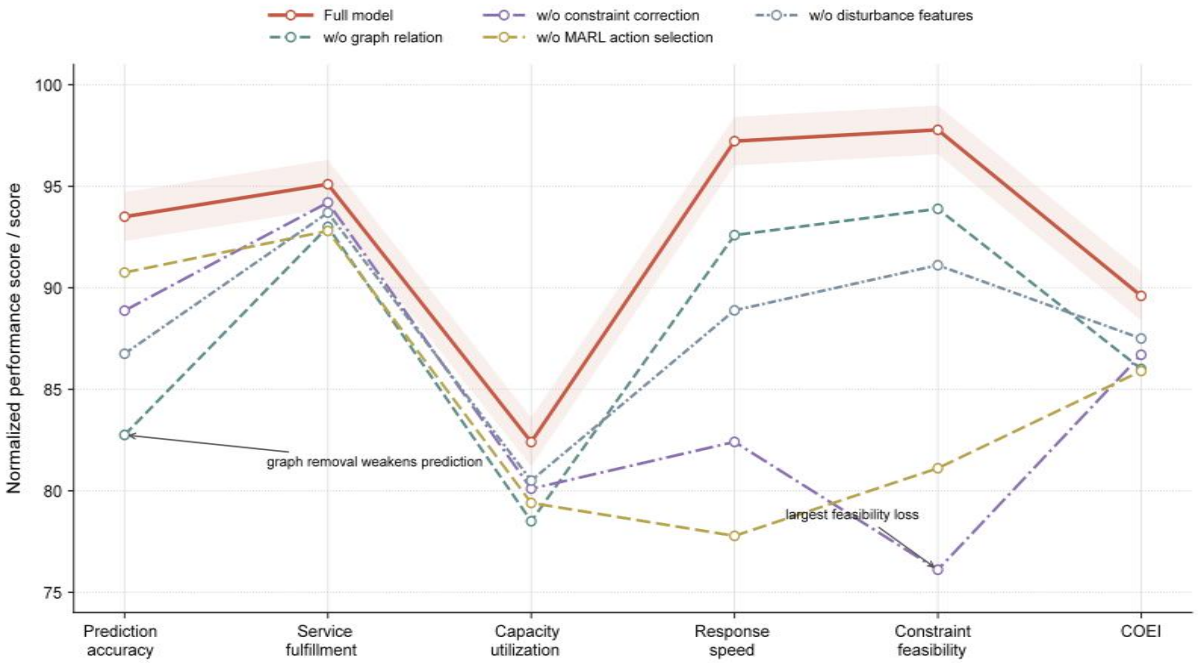

Figure 7: Ablation results of core model components.

In Figure 7, the prediction accuracy score decreases most significantly after removing graph relations, indicating that heterogeneous edge weights have a direct effect on node demand linkage identification. After removing constraint corrections, the constraint feasibility score decreases to the lowest while the response speed decreases, indicating that simply improving prediction accuracy does not guarantee that the solution is executable. After removing multi-intelligent body action selection, service fulfillment and response speed decrease simultaneously, indicating that the local action selection mechanism needs to be retained under cross-subject autonomy conditions. After removing the perturbation features, the overall COEI decreases less, but the decreases are more concentrated in weather and traffic-constrained scenarios, indicating that the perturbation features mainly support the robustness in extreme scenarios.

3.3 Efficiency frontier, error source and deployment implication

Collaborative optimization of the tourism supply chain needs to face the tension between service quality and operating costs at the same time. Excessive pursuit of service fulfillment may lead to high-frequency connectivity, platform subsidies, and rising temporary scheduling costs; and excessive cost compression may result in tourists waiting, node congestion, and idle service capacity. Smart tourism governance studies have emphasized that digital innovation and smart governance of destinations need to simultaneously deal with technological efficiency, subjective collaboration and public management boundaries [21-23]. Therefore, this paper further analyzes the relationship between service fulfillment rate and unit order synergy cost. The efficiency frontier between service fulfillment rate and unit order collaboration cost is shown in Figure 6.

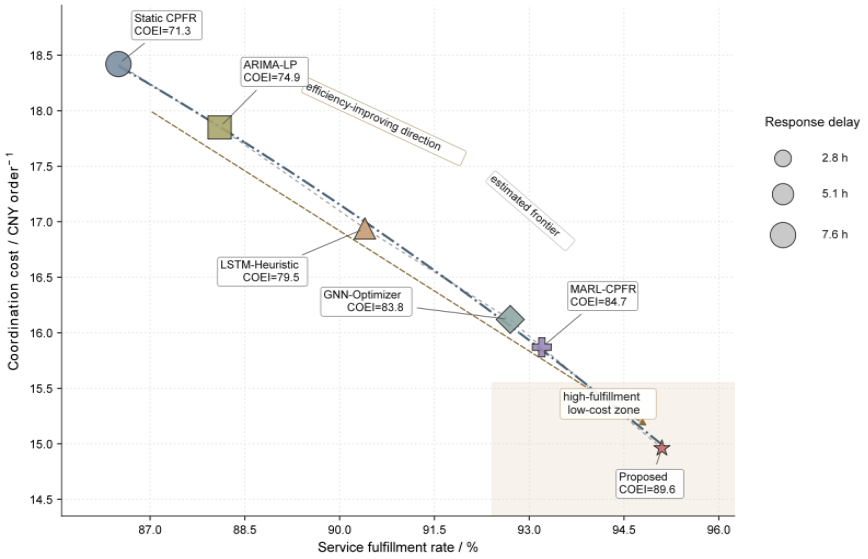

Figure 6: Ablation results of core model components.

In Fig. 6, Static CPFR is located in the upper left direction, with a service fulfillment rate of 86.5% and a unit order synergy cost of 18.42 CNY, which indicates that it has a higher cost of adjusting actions but limited service improvement.ARIMA-LP and LSTM-Heuristic are moving toward the efficiency frontier, but still suffer from large response delays.GNN-Optimizer and MARL-CPFR have entered the better region, reaching 92.7% and 93.2% respectively. GNN-Optimizer and MARL-CPFR have entered the better region, reaching 92.7% and 93.2% service compliance, respectively. The method in this paper is located in the lower right direction, the service fulfillment rate is 95.1%, the unit order collaboration cost is 14.96 CNY, and the bubble area is the smallest, which indicates that it achieves higher fulfillment, lower collaboration cost and shorter response delay at the same time. The change of node pressure and demand transfer path in the festival peak scenario is shown in Fig. 8.

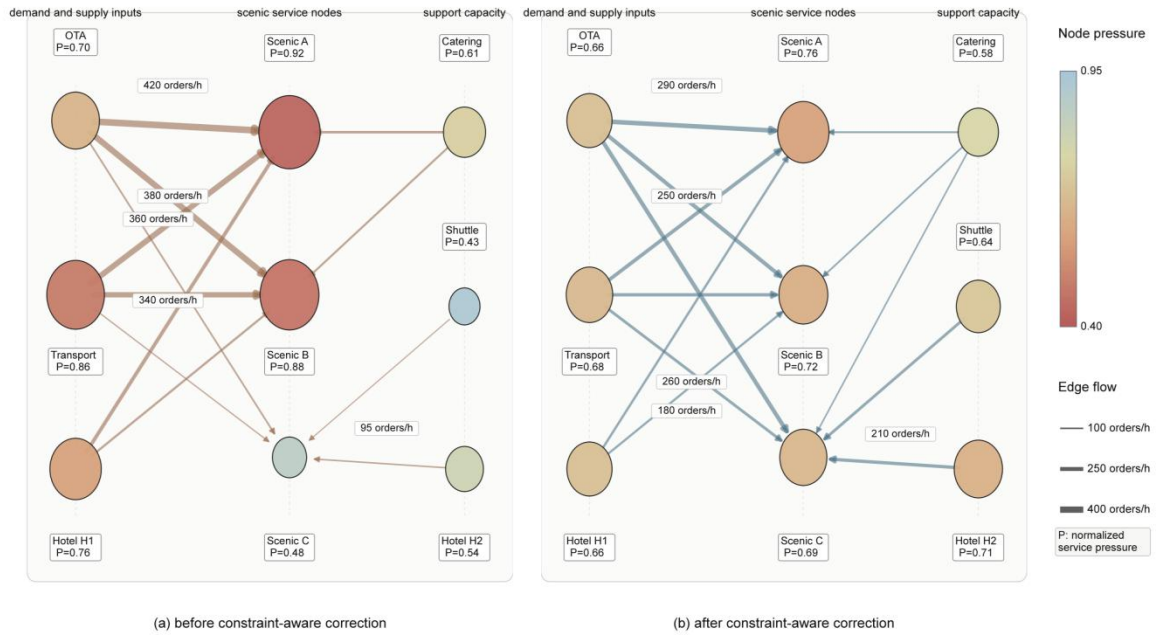

Figure 8: Ablation results of core model components.

In Fig. 8, the pressure indices of Scenic A, Scenic B and Transport hub before co-correction reach 0.92, 0.88 and 0.86, respectively, and the order flow of OTA reroute pointing to the core scenic spots is concentrated in the 380-420 orders h^{-1} area. After co-correction, Scenic C, Hotel H2 and Shuttle pool get more transfer demand, and the pressure of core scenic spots decreases to 0.76 and 0.72, and the pressure of Transport hub decreases to 0.68, which shows that the method in this paper doesn't simply compress the demand, but changes the path of the demand into the node through diversion, transportation connection and hotel capacity matching. Path.

The errors mainly come from three types of situations. First, unexpected events can cause non-linear jumps in tourist behavior, such as temporary concerts, social media outbreaks, and extreme weather warnings, and it is difficult to capture their full impact in time in a regular rolling window. Second, the real capacity of some supply chain nodes is characterized by soft constraints, e.g., hotels can temporarily add extra beds, scenic spots can extend opening hours, and catering companies can temporarily increase scheduling, and such elastic capacity is harder to accurately express in public data. Third, the platform recommendation strategy itself will reverse the distribution of tourist demand, so that the model faces the “predicted demand changed by the decision”. These errors suggest that an intelligent decision-making system for the tourism supply chain requires online feedback, strategy auditing, and manual backstopping mechanisms.

From the deployment point of view, this paper's method is suitable for embedding into destination integrated operation platforms, OTA resource scheduling systems, and holiday protection systems of cultural and tourism authorities. For destination operators, the model can be used to identify high-risk congestion nodes and generate cross-scenic diversion and transportation connection adjustment plans in advance.

For enterprises, the model can be used for linkage reservation of rooms, tickets, connections and catering capacity. For regulators, the model can provide early warning of capacity pressure under perturbation scenarios, and provide a basis for flow restriction, delayed service and traffic organization.The application of AI in tourism still needs to face transparency, sustainability and governance risks [24, 25], so the method in this paper should be used as an auxiliary decision-making tool. It is not appropriate to completely replace the manual emergency judgment when the data interface of the participating subjects is insufficient, the update of side rights is lagging behind, or there is a lack of real-time input for unexpected events.

4 Conclusion

This paper places emphasis on the optimization question of cooperative movement efficiency within travel supply chain, and therefore builds a smart decision-making method which combines different structure graph description, graph time sequence forecast, cooperative ability distribution and constraint-perceiving action adjustment. The experiment outcome shows the MAPE of the method in this paper is 6.52%, the rate of service fulfillment is 95.1%, the rate of capacity utilization is 82.4%, and COEI attains 89.6, which is 4.9 points higher than the best baseline, thus average response latency reduces by 28.2%.

(1) This paper organizes scenic spots, hotels, transportation, OTAs, food and beverage retailing and tourists' demand into a heterogeneous supply chain graph, and constructs dynamic side weights through transaction intensity, capacity complementarity, space time cost and disturbance risk, so that cross-principle synergistic relationships in the tourism supply chain can be explicitly exploited.

(2) In this paper, the forecast results are directly embedded into the synergistic allocation and action correction process. The model is able to more consistently translate forecasting accuracy into improvements in service fulfillment, capacity utilization, and cost control than

demand forecasting or static optimization-only approaches.

(3) The experiments in this paper are still based on public statistical data calibration and simulated operational samples, and have not yet covered enterprise-level real-time orders, dynamic pricing strategies, and individual tourist path data. Subsequent studies can introduce real platform logs, online learning and privacy-preserving co-training to improve the robustness of the model in cross-enterprise deployment.

About the Author

Fanfan Kong was born in Beijing, China, in 1988. She received her doctoral degree from City University of Macau. She is currently a lecturer at the School of Economics and Management, Binzhou Polytechnic. Her main research areas are tourism management and applied economics.

Junling Wen was born in Shandong, China, in 1973. She received her master's degree from Shandong Agricultural University. She is currently Dean of the School of Economics and Management at Binzhou Polytechnic and holds the title of Associate Professor. Her main research interests are economic management and financial management.

Huiqi Zhang was born in Lanzhou, Gansu Province, China, in 1987. She obtained her doctoral degree from City University of Macau and subsequently completed her postdoctoral research at Beijing Jiaotong University. Currently, she holds a position at Zhuhai City Polytechnic. Her research interests focus on green innovation, sustainable development, smart tourism, and consumer behavior.

References

[1] UN Tourism. (2026). World tourism barometer and statistical annex, January 2026. UN Tourism, 24(1).

[2] World Travel & Tourism Council. (2025). Travel & tourism economic impact research 2025. WTTC.

[3] OECD. (2024). Artificial intelligence and tourism: G7/OECD policy paper. OECD Tourism Papers, 2024(02).

[4] Ku, E. C. S. (2025). Tourism digital transformation and future supply chain competition: An integrated perspective on real options theory and digital competencies. Journal of Tourism Futures, 11(2), 240-260.

[5] Bekele, H., & Raj, S. (2025). Digitalization and digital transformation in the tourism industry: A bibliometric review and research agenda. Tourism Review, 80(4), 894-913.

[6] Luu, N. T. M., Pham, T. H., Siriwardana, A., et al. (2025). A bibliometric review of digitalization in tourism supply chains in the context of Industry 4.0. Strategic Change, 34(5), 577-595.

[7] Sarfraz, M., Khawaja, K. F., Han, H., et al. (2023). Sustainable supply chain, digital transformation, and blockchain technology adoption in the tourism sector. Humanities and Social Sciences Communications, 10, 557.

[8] Erol, I., Oztel, A., Dogru, T., et al. (2024). Supply chain resilience in the tourism and

hospitality industry: A comprehensive examination of driving and restraining forces. International Journal of Hospitality Management, 122, 103851.

[9] Zheng, J. (2025). Tourism supply chain resilience assessment and optimization based on complex networks and genetic algorithms. Systems and Soft Computing, 7, 200214.

[10] Liang, X., Li, X., Shu, L., et al. (2025). Tourism demand forecasting using graph neural network. Current Issues in Tourism, 28(6), 982-1001.

[11] Zhang, Y., Tan, W. H., & Zeng, Z. (2025). Tourism demand forecasting based on a hybrid temporal neural network model for sustainable tourism. Sustainability, 17(5), 2210.

[12] Ma, J. (2025). Demand forecasting of smart tourism integrating spatial metrology and deep learning. Scientific Reports, 15, 42646.

[13] Qin, F., Bi, J. W., Li, H., et al. (2025). Tourism demand forecasting using social media data: A deep learning-based ensemble model with social media communication conversion rates. Annals of Tourism Research, 115, 104058.

[14] Chen, J., Li, C., Huang, L., et al. (2025). Tourism demand forecasting: A deep learning model based on spatial-temporal transformer. Tourism Review, 80(3), 648-663.

[15] Kosasih, E. E., & Brintrup, A. (2022). A machine learning approach for predicting hidden links in supply chain with graph neural networks. International Journal of Production Research, 60(17), 5380-5393.

[16] Zheng, G., & Brintrup, A. (2025). A machine learning approach for enhancing supply chain visibility with graph-based learning. Supply Chain Analytics, 11, 100135.

[17] Mousa, M., van de Berg, D., Kotecha, N., et al. (2024). An analysis of multi-agent reinforcement learning for decentralized inventory control systems. Computers & Chemical Engineering, 188, 108783.

[18] Kim, B., Kim, J. G., & Lee, S. (2024). A multi-agent reinforcement learning model for inventory transshipments under supply chain disruption. IISE Transactions, 56(7), 715-728.

[19] Da Silva, G. A. F. R., Baierle, I. C., Gomes, L. C., et al. (2024). A comprehensive roadmap for connecting Industry 4.0 technologies to the basic model of collaborative planning, forecasting, and replenishment. Administrative Sciences, 14(6), 108.

[20] Hill, C. A., Zhang, G. P., & Miller, K. E. (2018). Collaborative planning, forecasting, and replenishment and firm performance: An empirical evaluation. International Journal of Production Economics, 196, 12-23.

[21] Ivars-Baidal, J., Casado-Díaz, A. B., Navarro-Ruiz, S., et al. (2024). Smart tourism city governance: Exploring the impact on stakeholder networks. International Journal of Contemporary Hospitality Management, 36(2), 582-601.

[22] Xu, J., Shi, P. H., & Chen, X. (2025). Exploring digital innovation in smart tourism destinations: Insights from 31 premier tourist cities in digital China. Tourism Review,

80(3), 681-709.

[23] Koo, C., Shin, S., Gretzel, U., et al. (2025). AI-powered smart tourism 2.0: A 10-year retrospective and updated model. Electronic Markets, 35, 108.

[24] Gössling, S., & Mei, X. Y. (2025). AI and sustainable tourism: An assessment of risks and opportunities for the SDGs. Current Issues in Tourism, 1-14.

[25] Tuo, Y., Wu, J., Zhao, J., et al. (2025). Artificial intelligence in tourism: Insights and future research agenda. Tourism Review, 80(4), 793-812.